Journal of Quality Measurement and Analysis *JQMA* 20(3) 2024, 181-198
e-ISSN: 2600-8602 *http://www.ukm.my/jqma*
https://doi.org/10.17576/jqma.2003.2024.13

PREDICTION OF COVID-19 TRANSMISSION BY SIRS MODEL USING 3-STEP PREDICTOR-CORRECTOR METHOD

(Peramalan Penularan COVID-19 Melalui Model SIRS Menggunakan Kaedah Peramal-Pembetul 3-langkah)

SALAUDEEN ABDULWAHEED ADEBAYO, SARATHA SATHASIVAM*,
MAJID KHAN BIN MAJAHAR ALI, CHEN CHU YI, LIM SHIN YING & MURALY VELAVAN

ABSTRACT

Effective and accurate prediction of the COVID-19 rate is vital for effective public health monitoring and intervention, but forecasting models are often hindered when it comes to striking a balance between accuracy and computing efficiency. This often calls for better prediction models that can effectively capture the dynamics of transmission and can serve as an important tool for healthcare policymaking. This study introduces a hybrid model combining the 3-step Adams-Bashforth-Moulton (ABM) method with the Runge-Kutta (RK4) method to analyze and forecast COVID-19 transmission rates in Malaysia. The hybrid model utilize the RK4 method for generating initial solutions and the ABM method for refining predictions, which is then used to solve the SIRS compartmental using Malaysia-specific COVID-19 data, including confirmed cases, recoveries, deaths, population size, and contact rates. The hybrid RK4-ABM model demonstrates enhanced accuracy in predicting COVID-19 transmission rates. By combining the computational efficiency of RK4 with the accuracy of ABM, the model delivers improved forecasting performance over time. The study will be of massive contribution to epidemiological research by demonstrating the RK4-ABM model's effectiveness in predicting COVID-19 transmission rates and providing valuable insights for healthcare policymakers in Malaysia. This hybrid RK4-ABM model shows potential for future epidemic modeling and forecasting, highlighting the importance of mathematical approaches in understanding and controlling pandemic impacts.

Keywords: epidemic model; Runge-Kutta 4th order; hybrid; Adam-Bashforth method

ABSTRAK

Ramalan yang berkesan dan tepat terhadap kadar COVID-19 adalah penting untuk pemantauan dan intervensi kesihatan awam yang berkesan, tetapi model peramalan sering mengalami masalah apabila wujud ketidakseimbangan antara ketepatan dan kecekapan pengkomputeran. Hal ini memerlukan model ramalan yang lebih baik yang dapat mengesan dinamik penularan dan kebolehfungsiaan sebagai alat penting untuk pelaksanaan dasar penjagaan kesihatan. Kajian ini memperkenalkan model hibrid yang menggabungkan kaedah 3-langkah Adams-Bashforth-Moulton (ABM) dengan kaedah Runge-Kutta (RK4) untuk menganalisis dan meramalkan kadar penularan COVID-19 di Malaysia. Model hibrid ini menggunakan kaedah RK4 untuk menjana penyelesaian awal dan kaedah ABM untuk ramalan saringan yang kemudiannya digunakan untuk menyelesaikan bahagian SIRS menggunakan data COVID-19 khusus di Malaysia, termasuk kes yang disahkan, pemulihan, kematian, saiz penduduk, dan kadar hubungan. Model RK4-ABM hibrid menunjukkan ketepatan yang baik dalam meramalkan kadar penularan COVID-19. Dengan menggabungkan kecekapan pengiraan RK4 dengan ketepatan ABM, model ini memberikan prestasi ramalan yang lebih baik dari masa ke semasa. Kajian ini akan memberi sumbangan besar dalam penyelidikan epidemiologi dengan menunjukkan keberkesanan model RK4-ABM dalam meramalkan kadar penularan COVID-19 dan memberikan pandangan yang berguna untuk pemantauan penjagaan kesihatan di Malaysia. Model RK4-ABM hibrid ini menunjukkan potensi untuk memodelkan

dan meramalkan epidemik yang akan datang, seterusnya menekankan kepentingan pendekatan matematik dalam memahami dan mengawal kesan pandemik.

Kata kunci: model epidemik; Runge-Kutta peringkat ke-4; hibrid; kaedah Adam-Bashforth

1. Introduction

Coronavirus disease (COVID-19), an infectious disease with severe acute respiratory syndrome that belongs to coronavirus 2 (SARS-CoV-2), was discovered in a sub-region of China, precisely Wuhan in the Hubei province, since its discovery in late 2019 (Zhou & Fan 2012), a scenario that earned it the popular name (COVID-19). By January 2020. It has become popular around the globe, and all hands were on the desk to understand its symptoms and non-medical prevention methods since it is new to the world. Quarantine and isolation are popular public health practices that are often deployed to prevent the spread of infectious disease during disease outbreaks. Most nations adopted these non-medical approaches with the ultimate goal of breaking the chain of transmission of COVID-19. Non-medical approaches significantly slowed disease spread, while scientists and medical personnel worked to understand transmission dynamics, develop treatments, and offer guidance on managing the disease. By May 20th, 2020, barely six months after its discovery, the disease had infested about 4,806,299 people and the world had recorded about 318,599 deaths related to the COVID-19 infection (Giri & Rana 2020).

Malaysia, due to its proximity and relations with China, was vulnerable to the COVID-19 outbreak. The country received its first warning when a case was detected in Singapore, and eight individuals with contact to that case were traced to Johor, Malaysia (Shah *et al.* 2020). The first confirmed COVID-19 case in Malaysia was reported on January 25, 2020. By the end of the first wave on February 15, 2020, 22 cases had been confirmed, largely traced back to the Singapore case (Hashim *et al.* 2021). The virus quickly spread across Malaysia, reaching 3,662 cases by April 5, 2020. A significant religious gathering at the Sri Petaling Mosque in late February to early March 2020 further fueled the surge in cases, with many infections believed to have been brought in by international attendees (Alsayed *et al.* 2020). Following two major incidents, the case linked to Singapore and the religious gathering at the Sri Petaling Mosque, the potential severity of the COVID-19 outbreak in Malaysia became evident. The virus spreads through infected droplets expelled during coughing, sneezing, and other forms of physical contact. Malaysia, unprepared for the pandemic, found itself in the midst of an outbreak fueled by asymptomatic carriers, including attendees from the mosque event and individuals who had contact with the index case. As a result, Malaysia became one of the hardest-hit Asian nations, with over 38,000 deaths and more than 5 million affected (Shah *et al.* 2020). Globally, COVID-19 has caused over 700 million illnesses and more than 6 million deaths as of January 30, 2023, making it one of the most significant threats humanity has faced. Despite ongoing efforts, the world is still grappling with the pandemic, as cases and deaths continue to rise.

Undoubtedly, knowing the infection's patterns of transmission, is one of the prominent stages required when modelling an infectious disease. Understanding epidemiological trends and investigating whether the methods for preventing outbreaks are effective are major determinants of mathematical model success (Camacho *et al.* 2015). Such research and analysis will benefit in estimating possibilities for future occurrences, quantifying the threat other countries pose, and facilitating the creation of alternate solutions (Abdalla *et al.* 2023).

Real-time analysis of this infectious disease may come with several obstacles and challenges. For instance, a lengthy incubation period may delay the onset of clinical symptoms, making it more difficult to discover and test for cases in a timely manner. It may also delay the assessment and confirmation of cases of infectious diseases. Mathematical modelling strategies can overcome these delays and uncertainty by explicitly including delays originating from the typical course of infections and reporting systems (Zou *et al.* 2020; Kraemer *et al.* 2016). These are some of the difficulties that mathematical models can readily address while utilizing parameters, and since they are generally accepted, they attract the interest of many scholars across many academic disciplines. After COVID-19 became a global concern, researchers across various fields united to develop effective strategies to combat the pandemic. This led to a surge in studies aimed at analyzing and predicting the virus's impact (Chen *et al.* 2020). Epidemiology, which focuses on investigating disease causes, spread, and potential management strategies, became a crucial area of research. Mathematics plays a key role in epidemiology, helping to identify disease dynamics and transmission patterns through data collection and analysis. Mathematical modeling, particularly using compartmental models, has a history of success in studying disease transmission. These models divide the population into compartments, with assumptions made about movement between them. For example, the susceptible-infective-susceptible (SIS) model tracks individuals who move from being susceptible to infected and then back to susceptible. Compartmental models have been used to study various diseases, including bacterial infections, helminth-borne diseases, and sexually transmitted infections like gonorrhea.

The most prominent compartmental model is SIR, an acronym for susceptible, infected, and removed. As a compartmental model, it divides the population into different compartments or sections based on their disease status. It has a very simple construction, and its analysis has been an inspiration for other compartmental models. Compartmental models received acceptance among mathematicians, and much of their success is attributed to Hethcote, 1976, 1978, and 1989 (Shah *et al.* 2020; Brauer 2017). In the SIR model, every individual is originally regarded as susceptible (S); after being infected, they transfer to the infected (I) compartment, where they are infectious and infect other individuals. Finally, after recovering or dying, they move to the Removed (R) compartment, where they are no longer susceptible to the disease and cannot spread it to others. In the SIRS, the agent can move back to susceptible group and continue with the trend. However, this movement of agents between these compartments is controlled by a set of defined differential equations involving the transmission rate and recovery rate. A compartmental model is often used to simulate the progression of the disease with respect to time and evaluate the impact of various interventions, such as vaccination, quarantine, and isolation. The SIR has also witnessed the proposal of other variants like SEIR (susceptible, exposed, infected, and recovered) and SIRD (susceptible, infected, recovered, deceased) (Viguerie *et al.* 2021), which incorporate additional features by compartmentalizing exposed individuals and deceased individuals, respectively.

However, in order to simulate genuine events and forecast the long-term behaviour of the infectious disease, several scientists and researchers have solved the compartmental model numerically to get numerical solutions of these models, such as the fourth-order Runge-Kutta method (Mohammed *et al.* 2021), the finite difference method (Chen *et al.* 2022), and the meshless local discrete Galerkin method (Asadi-Mehregan *et al.* 2023). However, there is no documentation of the 3-step predictor-corrector approach being used to simulate COVID-19 transmission. Several research studies have shown the effectiveness of using numerical

methods in solving compartmental models (Ahmed *et al.* 2020; Yang & Wang 2020). Numerical methods are generally effective when working with complex compartmental models that lack closed-form analytical solutions; they are mostly simple and provide an acceptable approximate solution when properly modelled (Tang *et al.* 2020). Many real-world epidemiological, ecological, and chemical models fall into this category. Numerical methods offer a pragmatic approach to approximating solutions for models. Previous attempts, such as (Akogwu & Fatoba 2022; Zhang *et al.* 2022), utilised explicit methods to solve the compartmental model for modelling the transmission of COVID-19. Palma and Mungkasi (2024) solve the SEIR model using fourth and fifth-order Runge-Kutta methods, and reported similarity in the results obtained in their proposed method and Ode45; this justified the feasibility of applying numerical solutions in solving compartmental models. However, we proposed a hybrid of Runge Kutta of order 4 method and the 3-step ABM predictor-corrector method to solve the SIRS compartmental model for a feasible solution and onward projection of the COVID-19 transmission in Malaysia. The hybrid model effectively captured the trends in COVID-19 real data, demonstrating its potential as a reliable numerical technique and forecasting tool. It will offer valuable insights for stakeholders managing disease outbreaks and serve as an additional resource in the field of epidemiology.

2. SIRS Model

In this study, the SIRS model is used to predict the spread of COVID-19 in Malaysia, SIRS is an extension of the susceptible-infectious-Removed (SIR) model, which is described as susceptible-infectious-Removed-Susceptible. The SIRS model divides the population into three compartments or groups: susceptible, infected, and recovered. Susceptible individuals are members of the population who are not immune to the disease and can be infected. Infected individuals are members of the population who have been exposed to the disease and are capable of transmitting it to others. Recovered individuals are those who have been infected with the disease and have subsequently recovered. They are no longer capable of transmitting the disease, but they may be immune to it (Salman *et al.* 2021). In using the SIRS model, we make the assumption that agents can only move in one direction between compartments. Susceptible people can contract the infection; infected people can recover, but recovered people cannot contract the infection again. The SIRS model is mostly used to forecast how many members of the population will be present in each compartment over time. The model can be deployed to evaluate how different measures, such as vaccination and quarantine, will affect the disease's transmission. The SIRS model is simple, effective, and offers a quick understanding of disease transmission. Thus, the SIRS model is also based on some restrictions, which include homogeneity of the population and the assumption of constant rate infection. In this research, N is used to represent the total populations, which is made up of three compartments: the susceptible population denoted by $S(t)$, the infected population denoted $I(t)$ and, the removal class represented by $R(t)$ which is made up of recovered and death cases.

3. Mathematical Formulation of SIRS Model

The mathematical formulation framework used in this study is based on the type of SIRS model that describes the incorporation effects of different epidemiological parameters on COVID-19 outbreaks, such as the lack of medical resources, interaction rate and the potential for reinfection, among others, as described in (Mohd & Sulayman 2020; Salman *et al.* 2021).

$$\frac{dS}{dt} = \eta N - \frac{\delta SI}{N} + \varepsilon R - \nu S \tag{1}$$

$$\frac{dI}{dt} = \frac{\delta SI}{N} - (\psi + \nu) I - \frac{\rho I}{\phi + I} \tag{2}$$

$$\frac{dR}{dt} = \psi I + \frac{\rho I}{\phi + I} - (\varepsilon + \upsilon) R \tag{3}$$

where N denotes the total population and it is calculated using $N = S + I + R$, where S denotes the susceptible population, I denotes the infected population, and R represents the removed population (recovered or dead). In Eqs. (1)-(3) above, η denotes the birth rate, δ is transmission rate, ε denotes the reinfection rate, ν represent the death rate, ψ is recovery rate from the diseases. Since we are dealing with the SIRS compartmental model, it can be assumed that a small fraction of recovered individuals from the removal class can re-enter the susceptible compartment with a rate of ε and that this rate corresponds to the reinfection rate. This will assist our model to capture the necessary information regarding the COVID-19 transmission dynamics, since there is no evidence of developing immunity against COVID-19. However, the term $(\rho I/\phi + I)$ can be used to demonstrate the effects of the COVID-19 outbreak in restricted or limited medial resources (Zhou & Fan 2012) . ρ denotes the medical resources available per unit time and ϕ is half-saturation constant (Salman *et al.* 2021). This quantity represents the efficiency of the supply of medical resources, and this situation would depend on other factors like control strategies (such as movement control orders, quarantine), the supply of drugs and vaccines among other factors. Half-saturation constant is frequently used in disease modeling. It plays an important role in modelling the dynamics of interactions between populations, resources, and limiting factors. In disease modelling, the half-saturation coefficient is associated with models that involve the transmission and growth of infectious diseases within a population (Mohd & Sulayman 2020). The parameters used in this research are all assumed to be non-negative to efficiently suit COVID-19 transmission dynamics.

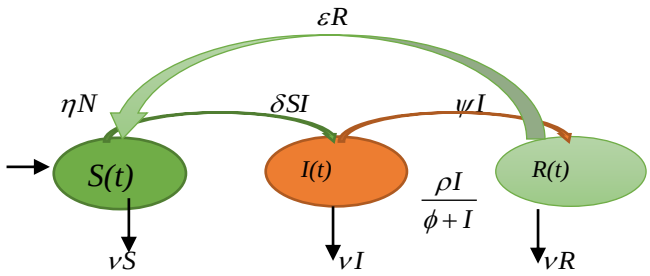

Figure 1: 1Illustration of the movement of agents within the SIRS model

4. Runge-Kutta Fourth Order (RK4)

Runge-Kutta 4th order (RK4), a popular numerical method, is an explicit method that is used to numerically solve the initial-value problems of first-order ordinary differential equations

(ODE) (Akinsola 2023). A differential equation of the form in Eq. (4) is an example of a first-order ODE that can be solved using the RK4 formula shown in Eq. (5).

$$\frac{dy}{dx} = f(x, y)\,,\ y(x_0) = y_0\,, \tag{4}$$

$$y_{n+1} = y_n + \frac{h}{6}\left(k_1 + 2k_2 + 2k_3 + k_4\right) \tag{5}$$

where $n = 0, 1, 2, \ldots, h$ is the step size, $y(x_0) = y_0$ denotes the initial condition and k_i are intermediate slopes and they are defined as:

$$\begin{aligned}
k_1 &= f(t_i, y_i),\\
k_2 &= f\left(t_i + \frac{h}{2}, y_i + \frac{hk_1}{2}\right)\\
k_3 &= f\left(t_i + \frac{h}{2}, y_i + \frac{hk_2}{2}\right)\\
k_4 &= f\left(t_i + h, y_i + hk_3\right).
\end{aligned}$$

By modifying the first order ODE in Eq. (4) to accommodate system of ODE we have:

$$\frac{dS}{dt} = f_s(t, S, \mathrm{I}, \mathrm{R})\ \frac{dI}{dt} = f_I(t, S, \mathrm{I}, \mathrm{R})\ \frac{dR}{dt} = f_R(t, S, \mathrm{I}, \mathrm{R})\,, K_i^p \text{ for } P = S, I, R \text{ and } i = 1, 2, 3, 4$$

where S denotes susceptible population, I denotes infected population and R denotes as removal class. Taking $h = 1$ as the step size and $n = 0, 1, 2$. We transformed the RK4 in term of SIRS compartmental model as:

For the susceptible population we have:

$$S_{n+1} = S_n + \frac{h}{6}\left(k_1^s + 2k_2^s + 2k_3^s + k_4^s\right). \tag{6}$$

where

$$\begin{aligned}
k_1^s &= f_s(t_n, S_n, \mathrm{I}_n, \mathrm{R}_n) = \eta\,\mathrm{N} - \frac{\delta\,\mathrm{S}_n\, I_n}{N} + \varepsilon R_n - \nu S_n\,,\\
k_2^s &= f_s\left(t_n + \frac{1}{2}\mathrm{h}, S_n + \frac{1}{2}\mathrm{h}\,k_1^s, \mathrm{I}_n + \frac{1}{2}\mathrm{h}\,k_1^I, \mathrm{R}_n + \frac{1}{2}\mathrm{h}\,k_1^R\right) = \eta\,\mathrm{N} - \frac{\delta\left(\mathrm{S}_n + \frac{1}{2}\mathrm{h}\,k_1^s\right)\left(I_n + \frac{1}{2}\mathrm{h}\,k_1^I\right)}{N}\\
&\quad + \varepsilon\left(R_n + \frac{1}{2}\mathrm{h}\,k_1^R\right) - \nu\left(S_n + \frac{1}{2}\mathrm{h}\,k_1^s\right),
\end{aligned}$$

$$k_3^s = f_s(t_n + \frac{1}{2}\mathrm{h}, S_n + \frac{1}{2}\mathrm{h}\,k_2^s, \mathrm{I}_n + \frac{1}{2}\mathrm{h}\,k_2^I, \mathrm{R}_n + \frac{1}{2}\mathrm{h}\,k_2^R) = \eta\,\mathrm{N} - \frac{\delta\left(\mathrm{S}_n + \frac{1}{2}\mathrm{h}\,k_2^s\right)\left(I_n + \frac{1}{2}\mathrm{h}\,k_2^I\right)}{N} + \varepsilon\left(R_n + \frac{1}{2}\mathrm{h}\,k_2^R\right) - \nu\left(S_n + \frac{1}{2}\mathrm{h}\,k_2^s\right),$$

$$k_4^s = f_s(t_n + \mathrm{h}, S_n + \mathrm{h}\,k_3^s, \mathrm{I}_n + \mathrm{h}\,k_3^I, \mathrm{R}_n + \mathrm{h}\,k_3^R) = \eta\,\mathrm{N} - \frac{\delta\left(\mathrm{S}_n + \mathrm{h}\,k_3^s\right)\left(I_n + \mathrm{h}\,k_3^I\right)}{N} + \varepsilon\left(R_n + \mathrm{h}\,k_3^R\right) - \nu\left(S_n + \mathrm{h}\,k_3^s\right).$$

For infected population we have;

$$I_{n+1} = I_n + \frac{h}{6}\left(k_1^I + 2k_2^I + 2k_3^I + k_4^I\right). \tag{7}$$

where

$$k_1^I = f_I(t_n, S_n, \mathrm{I}_n, \mathrm{R}_n) = \frac{\delta\,\mathrm{S}_n\,I_n}{N} - (\psi + \nu)\,I_n - \frac{\rho I_n}{\phi + I_n},$$

$$k_2^I = f_I(t_n + \frac{1}{2}\mathrm{h}, S_n + \frac{1}{2}\mathrm{hk}_1^s, \mathrm{I}_n + \frac{1}{2}\mathrm{hk}_1^I, \mathrm{R} + \frac{1}{2}\mathrm{hk}_{1\,n}^R)$$

$$= \frac{\delta\left(\mathrm{S}_n + \frac{1}{2}\mathrm{hk}_1^s\right)\left(I_n + \frac{1}{2}\mathrm{hk}_1^I\right)}{N} - (\psi + \nu)\left(I_n + \frac{1}{2}\mathrm{hk}_1^I\right) - \frac{\rho\left(I_n + \frac{1}{2}\mathrm{hk}_1^I\right)}{\phi + \left(I_n + \frac{1}{2}\mathrm{hk}_1^I\right)},$$

$$k_3^I = f_I(t_n + \frac{1}{2}\mathrm{h}, S_n + \frac{1}{2}\mathrm{hk}_2^s, \mathrm{I}_n + \frac{1}{2}\mathrm{hk}_2^I, \mathrm{R}_n + \frac{1}{2}\mathrm{hk}_2^R) = \frac{\delta\left(\mathrm{S}_n + \frac{1}{2}\mathrm{hk}_2^s\right)\left(I_n + \frac{1}{2}\mathrm{hk}_2^I\right)}{N} - (\psi + \nu)\left(I_n + \frac{1}{2}\mathrm{hk}_2^I\right) - \frac{\rho\left(I_n + \frac{1}{2}\mathrm{hk}_2^I\right)}{\phi + \left(I_n + \frac{1}{2}\mathrm{hk}_2^I\right)},$$

$$k_4^I = f_I(t_n + \mathrm{h}, S_n + \mathrm{hk}_3^s, \mathrm{I}_n + \mathrm{hk}_3^I, \mathrm{R}_n + \mathrm{hk}_3^R) = \frac{\delta\left(S_n + \mathrm{hk}_3^s\right)\left(I_n + \mathrm{hk}_3^I\right)}{N} - (\psi + \nu)\left(I_n + \mathrm{hk}_3^I\right) - \frac{\rho\left(I_n + \mathrm{hk}_3^I\right)}{\phi + \left(I_n + \mathrm{hk}_3^I\right)}.$$

For the recovered population we have:

$$R_{n+1} = R_n + \frac{h}{6}\left(k_1^R + 2k_2^R + 2k_3^R + k_4^R\right). \tag{8}$$

where,

$$k_1^R = f_R(t_n, S_n, \mathrm{I}_n, \mathrm{R}_n) = \psi I_n + \frac{\rho I_n}{\phi + I_n} - (\varepsilon + \nu)\mathrm{R}_n,$$

$$k_2^R = f_I\left(t_n + \frac{1}{2}\mathrm{h}, S_n + \frac{1}{2}\mathrm{hk}_1^s, \mathrm{I}_n + \frac{1}{2}\mathrm{hk}_1^I, \mathrm{R}_n + \frac{1}{2}\mathrm{hk}_1^R\right) = \psi\left(I_n + \frac{1}{2}hk_1^I\right) + \frac{\rho\left(I_n + \frac{1}{2}\mathrm{hk}_1^I\right)}{\phi + \left(I_n + \frac{1}{2}\mathrm{hk}_1^I\right)} - (\varepsilon + \upsilon)\left(R_n + \frac{1}{2}hk_1^R\right),$$

$$k_3^R = f_I\left(t_n + \frac{1}{2}\mathrm{h}, S_n + \frac{1}{2}\mathrm{hk}_2^s, \mathrm{I}_n + \frac{1}{2}\mathrm{hk}_2^I, \mathrm{R}_n + \frac{1}{2}\mathrm{hk}_2^R\right) = \psi\left(I_n + \frac{1}{2}hk_2^I\right) + \frac{\rho\left(I_n + \frac{1}{2}\mathrm{hk}_2^I\right)}{\phi + \left(I_n + \frac{1}{2}\mathrm{hk}_2^I\right)} - \left(R_n + \frac{1}{2}hk_2^R\right),$$

$$k_4^R = f_R(t_n + \mathrm{h}, S_n + h\,\mathrm{k}_3^s, \mathrm{I}_n + \mathrm{hk}_3^I, \mathrm{R}_n + \mathrm{hk}_3^R) = \psi(I_n + hk_3^I) + \frac{\rho\left(I_n + \mathrm{hk}_3^I\right)}{\phi + \left(I_n + \mathrm{hk}_3^I\right)} - (\varepsilon + \upsilon)\left(R_n + hk_3^R\right).$$

Hence, with known values of $S(0) = \mathrm{S}_0$, $I(0) = I_0$ and $R(0) = R_0$ we obtain the numerical solution of $S(t)$, $I(t)$ and $R(t)$ for t = 1 day and t = 2 day can be obtained using Eqs. (4)-(6). However, the choice of time step size h is one of the factors that influences the quality of the solution using the Runge-Kutta method; it also has a significant impact on the accuracy of the numerical integration. It had been established that a smaller time step size provided a more accurate approximation of the solution at the expense of more computational time. The calculation of the value of k_i involves computation sub-step size within the original step size. k_i represents how the function changes at different points within the time step. This is one of the factors that makes the Runge-Kutta method stand out among non-multistep methods, as small step sizes mean smaller sub-step sizes, leading to a more accurate result.

5. 3-step Predictor-Corrector Method

This study utilises the 3-step Adams-Bashforth method as a predictor and Adams-Moulton 3-step method as a corrector to solve the SIRS model. Both the 3-step Adams-Bashforth method and the Adams-Moulton 3-step method are multistep method numerical method. 3-step predictor-corrector method, is a mixture of both explicit and implicit methods, which is responsible for its stability and accuracy. The explicit section is used to find the next solution, while in the implicit section, the trend is repeated until the required accuracy is reached. Since only one initial value is needed in the SIRS model, the RK4 method is employed to find the second and third points. We then applied the 3-step Adams-Bashforth method and 3-step Adams-Moulton method. The mathematical representation of 3-step Adams-Bashforth method as shown in Eq. (9) and Eq. (10).

- 3-step Adams-Bashforth method:

$$y_{n+1}^{p} = y_n + \frac{h}{12}\left[23f(x_n, y_n) - 16f(x_{n-1}, y_{n-1}) + 5f(x_{n-2}, y_{n-2})\right]. \tag{9}$$

- 3-step Adams-Moulton method:

$$y_{n+1}^{c} = y_n + \frac{h}{12}\left[5f(x_{n+1}, y_{n+1}^{p}) + 8f(x_n, y_n) - f(x_{n-1}, y_{n-1})\right]. \tag{10}$$

We transform Eq. (9) and Eq. (10) to suit our SIRS model, as shown in Eqs. (11)–(13). However y_{n+1}^{p} is replaced by S_{n+1}^{p}, I_{n+1}^{p} and R_{n+1}^{p}. While y_{n+1}^{c} is replace by S_{n+1}^{c}, I_{n+1}^{c} and R_{n+1}^{c}

$$\begin{aligned} S_{n+1}^{p} &= S_n + \frac{h}{2}\left[23f_s(t_n, \mathrm{S}_n, \mathrm{I}_n, \mathrm{R}_n) - 16f_s(t_{n-1}, \mathrm{S}_{n-1}, \mathrm{I}_{n-1}, \mathrm{R}_{n-1}) + 5f_s(t_{n-2}, \mathrm{S}_{n-2}, \mathrm{I}_{n-2}, \mathrm{R}_{n-2})\right] \\ &= S_n + \frac{h}{2}\left(\begin{array}{l} 23\left[\eta \mathrm{N} - \dfrac{\delta \mathrm{S}_n I_n}{N} + \varepsilon R_n - \nu S_n\right] - 16\left[\eta \mathrm{N} - \dfrac{\delta \mathrm{S}_{n-1} I_{n-1}}{N} + \varepsilon R_{n-1} - \nu S_{n-1}\right] \\ + 5\left[\eta \mathrm{N} - \dfrac{\delta \mathrm{S}_{n-2} I_{n-2}}{N} + \varepsilon R_{n-2} - \nu S_{n-2}\right] \end{array}\right) \end{aligned} \tag{11}$$

$$\begin{aligned} I_{n+1}^{p} &= I_n + \frac{h}{12}\left[23f_I(t_n, S_n, I_n, R_n) - 16f_I(t_{n-1}, S_{n-1}, I_{n-1}, R_{n-1}) + 5f_I(t_{n-2}, S_{n-2}, I_{n-2}, R_{n-2})\right] \\ &= I_n + \frac{h}{12}\left[\begin{array}{l} 23\left[\dfrac{\delta \mathrm{S}_n I_n}{N} - (\psi + \nu) I_n - \dfrac{\rho I_n}{\phi + I_n}\right] - 16\left[\dfrac{\delta \mathrm{S}_{n-1} I_{n-1}}{N} - (\psi + \nu) I_{n-1} - \dfrac{\rho I_{n-1}}{\phi + I_{n-1}}\right] \\ +5\left[\dfrac{\delta \mathrm{S}_{n-2} I_{n-2}}{N} - (\psi + \nu) I_{n-2} - \dfrac{\rho I_{n-2}}{\phi + I_{n-2}}\right] \end{array}\right] \end{aligned} \tag{12}$$

$$\begin{aligned} R_{n+1}^{p} &= R_n + \frac{h}{12}\left[23f_R(t_n, S_n, I_n, R_n) - 16f_R(t_{n-1}, S_{n-1}, I_{n-1}, R_{n-1}) + 5f_R(t_{n-2}, S_{n-2}, I_{n-2}, R_{n-2})\right] \\ &= R_n + \frac{h}{12}\left(\begin{array}{l} 23\left[\psi I_n + \dfrac{\rho I_n}{\phi + I_n} - (\varepsilon + \nu)\mathrm{R}_n\right] - 16\left[\psi I_{n-1} + \dfrac{\rho I_{n-1}}{\phi + I_{n-1}} - (\varepsilon + \nu)\mathrm{R}_{n-1}\right] \\ +5\left[\psi I_{n-2} + \dfrac{\rho I_{n-2}}{\phi + I_{n-2}} - (\varepsilon + \nu)\mathrm{R}_{n-2}\right] \end{array}\right) \end{aligned} \tag{13}$$

The corresponding 3-step Adams-Moulton method (corrector) are modified as shown in Eqs. (14)-(16).

$$\begin{aligned} S_{n+1}^{c} &= S_n + \frac{h}{2}\left[5f_s(t_{n+1}, \mathrm{S}_{n+1}^{p}, \mathrm{I}_{n+1}^{p}, \mathrm{R}_{n+1}^{p}) + 8f_s(t_n, \mathrm{S}_n, \mathrm{I}_n, \mathrm{R}_n) - f_s(t_{n-1}, \mathrm{S}_{n-1}, \mathrm{I}_{n-1}, \mathrm{R}_{n-1})\right] \\ &= S_n + \frac{h}{2}\left(\begin{array}{l} 5\left[\eta \mathrm{N} - \dfrac{\delta \mathrm{S}_{n+1}^{p} I_{n+1}^{p}}{N} + \varepsilon R_{n+1}^{p} - \nu S_{n+1}^{p}\right] + 8\left[\eta \mathrm{N} - \dfrac{\delta \mathrm{S}_n I_n}{N} + \varepsilon R_n - \nu S_n\right] \\ - \left[\eta \mathrm{N} - \dfrac{\delta \mathrm{S}_{n-1} I_{n-1}}{N} + \varepsilon R_{n-1} - \nu S_{n-1}\right] \end{array}\right) \end{aligned} \tag{14}$$

$$I_{n+1}^{c} = I_n + \frac{h}{12}\left[5 f_I(t_{n+1}, S_{n+1}^{p}, I_{n+1}^{p}, R_{n+1}^{p}) + 8 f_I(t_n, S_n, I_n, R_n) - f_I(t_{n-1}, S_{n-1}, I_{n-1}, R_{n-1})\right]$$

$$= I_n + \frac{h}{12}\left(\begin{array}{l} 5\left[\dfrac{\delta \mathrm{S}_{n+1}^{p} I_{n+1}^{p}}{N} - (\psi+\nu) I_{n+1}^{p} - \dfrac{\rho I_{n+1}^{p}}{\phi + I_{n+1}^{p}}\right] + 8\left[\dfrac{\delta \mathrm{S}_n I_n}{N} - (\psi+\nu) I_n - \dfrac{\rho I_n}{\phi + I_n}\right] \\ -\left[\dfrac{\delta \mathrm{S}_{n-1} I_{n-1}}{N} - (\psi+\nu) I_{n-1} - \dfrac{\rho I_{n-1}}{\phi + I_{n-1}}\right] \end{array}\right) \tag{15}$$

$$R_{n+1}^{c} = R_n + \frac{h}{12}\left[5 f_I(t_{n+1}, S_{n+1}^{p}, I_{n+1}^{p}, R_{n+1}^{p}) + 8 f_I(t_n, S_n, I_n, R_n) - f_I(t_{n-1}, S_{n-1}, I_{n-1}, R_{n-1})\right]$$

$$= R_n + \frac{h}{12}\left(\begin{array}{l} 5\left[\psi I_{n+1}^{p} + \dfrac{\rho I_{n+1}^{p}}{\phi + I_{n+1}^{p}} - (\varepsilon+\nu)\mathrm{R}_{n+1}^{p}\right] + 8\left[\psi I_n + \dfrac{\rho I_n}{\phi + I_n} - (\varepsilon+\nu)\mathrm{R}_n\right] \\ -\left[\psi I_{n-1} + \dfrac{\rho I_{n-1}}{\phi + I_{n-1}} - (\varepsilon+\nu)\mathrm{R}_{n-1}\right] \end{array}\right) \tag{16}$$

Therefore, the numerical solution of S, I and R, are S_{n+1}^{c}, I_{n+1}^{c} and R_{n+1}^{c} respectively for value of $n = 3,4,5\ldots$ solving the differential equations numerically involves specifying the initial conditions for each of the variables in the compartments. An appropriate time step is chosen to control how updates should be done in each iteration, and the values of are updated as the time increases to the desired number of years.

6. Data Source, System and Software Requirement

The extracted data is from December 1, 2020, until January, 2021. The data is made cumulative to compare with the numerical results. We examined the infection of COVID-19 using our proposed model for long-term predictions in instances where there are limited medical resources and chances of reinfection (SIRS model). Real COVID-19 data released by the Ministry of Health Malaysia (MOH) that include demographic data (location, age, and gender, nature of contact between individuals in the community). Other relevant features used in the model were adopted from Salman *et al.* (2021). The parameter values and initial conditions provided in Salman *et al.* (2021) were equally adopted. The daily number of active cases and removed cases provided by the Ministry of Health (MOH) is extracted from Dong *et al.* (2020). We equally adopted similar parameterization of the COVID-19 active cases data from Malaysia. Even though we opted for value of $\rho = 0$ which indicate the absence of medical facilities or efficiency , we intentionally neglect the effect of medical intervention such as vaccination and stick to non-medical practices like isolation, quarantine, social distancing, and other means that could lower the transmission rate of COVID-19 among people without including the purchase of any materials. The parameterization employed provided us with credible components of the model, such as transmission rate, recovery rate, mortality rate, as well as the incubation period of COVID-19, while the data has its cradle from the Ministry of Health Malaysia.

To effectively implement our model, we deployed the use of the MATLAB programming language to reduce the computational burden. MATLAB was chosen as an appropriate programming language in our studies because it came with a wide range of scientific libraries and tools for data analysis and effective stimulation; we utilised the 2022a version. It was

deployed mainly to ease the computational burden for better accuracy as well as result analysis. We exploited its various built-in functions and commands in the coding development phase and utilized it in the code development of RK4, the 3-step Adams-Bashforth method, and the 3-step Adams-Moulton method to solve the SIRS model, and we equally used Microsoft Excel to visualize the numerical results and make comparisons with the actual data.

7. Flowchart of The Proposed Hybrid Model and Its Description

Figure 2 shows the flowchart outlining the step-by-step process of the proposed hybrid model, illustrating the sequence of methods applied and the conncetion between the Runge-Kutta and Adams-Bashforth-Moulton methods in forecasting COVID-19 transmission rates.

- Step 1: We define the compartmental model by identifying the type of compartments that suits the problem we want to model. This is followed by the description of a differential equations that can capture the exchange of entities between the compartments using the model dynamics. With all the equations that made up our compartmental model and availability of the parameters needed as stated in Table 1.
- Step 2: We implement the RK4 method. It begins by setting initial conditions for each of the compartments, which include the number of susceptible, infected, and recovered individuals at initial time (t_o). The compartmental model is presented as a system of first-order ordinary differential equations (ODEs).
- Step 3: The implementation of the RK4 method is basically to numerically solve the ODE system. This involves dividing the time interval into discrete steps using the k_i $(i = 1, 2, 3, 4)$ and iteratively updating the compartment values using intermediate calculations. The specification of time span and step size is also done here. We initialize arrays or data structures to store the compartment values at each time step. Iterate over the time steps, using the RK4 method to update the compartment values at each step. The compartment values at each time step are stored for further utilisation, after obtaining the first three solutions from RK4, which is S_1, S_2 and S_3 , I_1, I_2 and I_3 and R_1, R_2 and R_3 for susceptible, infected and removed respectively, while S_1, I_1 and R_1 are set as initial condition to match the indexing format in MATLAB.
- Step 4: We initialise Adams-Bashforth predictor-corrector method with the values obtained from the RK4 solutions. The 3-step Adams-Bashforth predictor-corrector method is deployed mainly to further refine the solutions, being an implicit method, it can lead to an increase in stability and improve accuracy. Specifications of the time span and step size are set for the stimulation. The time span begins with 4, taking into cognizance that the few solutions have been obtained using the RK4 method, and we initialise arrays to store the compartment values at each time step.
- Step 5: We iterate over the time steps through the 3-step Adams-Bashforth predictor-corrector method. Using 3- step Adams-Bashforth predictor to predict the solution and 3-step Adams-Morton corrector for possible refinement, we update the compartment values at each time step based on the refined predictions.
- Step 6: The iteration is terminated on reaching the desired time span, and the graphs of the solutions are plotted based on the results obtained in the step 5 above, We then analysed the results of the hybrid model while comparing the results of the model with the real data of COVID-19 within the stipulated time frame.

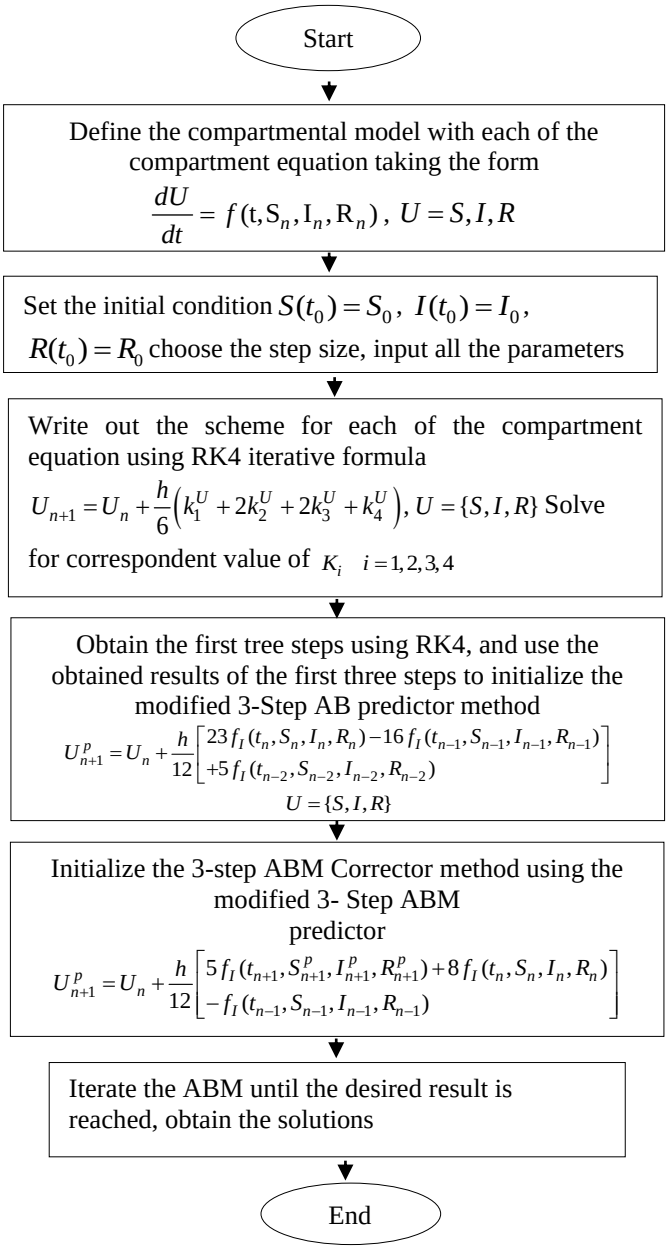

Figure 2: Flowchart showing the proposed method

However, the hybrid of RK4 and 3-step ABM predictor-corrector method can be deployed to predict the COVID-19 transmission at each time step by expressing each of the compartmental equations as a scheme that can be solved iteratively, thus Eq. (10) can be used as corresponding schemes for the susceptible, infected, and removed classes. Once the solution at the time $(t-1)$ is known, we can easily compute the solution at the time (t) and beyond. The hybrid model benefits from the RK4 method's explicit nature and high-order accuracy, which makes it efficient and accurate for most situations but suffers when the system exhibits stiff behaviour. ABM is used as a stabiliser of the solution during stiff phases,

as it can handle stiff ODEs more effectively than RK4. This will leverage their respective strengths by improving accuracy, adapting to the dynamical nature of compartmental models, and reducing computational overhead. Having a previous solution, the present solution can be obtained, which can be used to generate future solutions that represent a trend in the dataset.

8. Result and Discussion

Parameterization of the COVID-19 active cases daily data from Malaysia from December 1, 2020 to January 31, 2021 shown in Table 1, was extracted from (Salman *et al.* 2021).

Table 1: Parameters used in the simulation

Description	Parameters	Value
Half- saturated constant	ϕ	3.0173
Medical resources per unit time	ρ	0
Reinfection rate	ε	0.00032422
Recovery rate	ψ	0.026
Transmission rate	δ	0.11
Death rate	υ	0.00002
Birth rate	η	0.000006
Total population	N	185975
Susceptible Population	$S(0)$	119,169
Infected population	$I(0)$	10,495
Removal population	$R(0)$	56,311

Information presented in Table 1 was utilised in order to investigate and predict the transmission rate of COVID-19 in Malaysia within the specified period of days. The parameter values were utilized in our proposed hybrid for the period of 2000 days since we target long-term predictions in instances where there are limited supplies of medical resources such as vaccines, drugs, hospital beds, ventilators, testing kits, and other advanced medical equipment. The research strictly focused on transmission based on non-medical practises like quarantine, isolation, social distance, and other non-medical practices that can retard the spread of diseases among the populace. The model was used to find the solutions of $S(t)$, $I(t)$ and $R(t)$ for everyday in the interval of 2000 days, and the results were presented in the graph below and compare with the actual infection rate as shown in Figure 3.

Figure 3 illustrates the predicted dynamics of COVID-19 transmission using the hybrid of RK4 and 3-step ABM predictor- corrector method in a compartmental model (SIRS) which accounts for susceptible individuals (S), infected individuals (I), and recovered individuals (R) over time (in days). The graph compares predicted results with actual COVID-19 cases which are concentrated on the left side of the graph, justifying that the actual data covers a limited period (around the first 50 days), it shows a sharp increase initially before stabilizing.

Recovery curve exhibits a sharp increase initially, peaking near 16,000 cases, it then decline gradually. After a significant decrease, it rises again around day 1,400, indicating a possible resurgence of recoveries due to reinfection or second waves of the pandemic. Infected population curve starts with a sharp rise, reaching a peak early in the pandemic, it then declines steadily and flattens out after around day 1,000, indicating a decrease in active infections. However, there are small subsequent peaks, possibly indicating intermittent surges or secondary waves of infections. This finding aligns with some experts findings and suggestions that new waves of infection may rise gradually and may be brought on by declining immunity (Kissler *et al.* 2020). Moreover, the number of COVID-19 infected cases

increases less steeply in future waves of outbreaks. Hence, despite the possibility of reinfection, this provides reassurance that our healthcare systems will not be overburdened in the future as they have in the past.

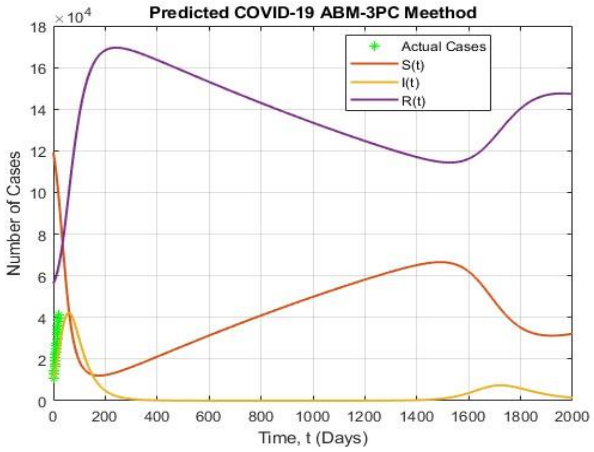

Figure 3: Numerical results of the SIRS model compares with the active cases in Malaysia

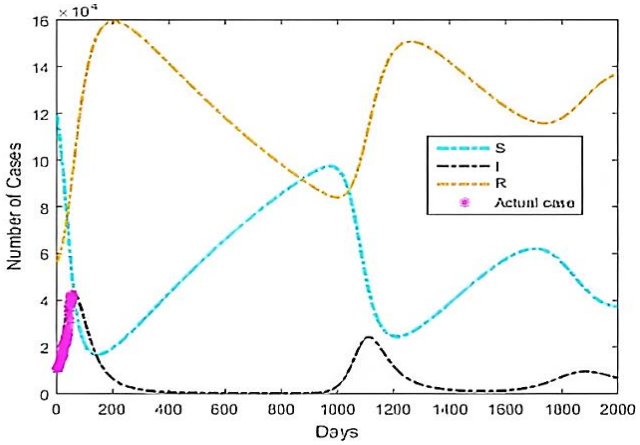

Figure 4: Results obtain for comparison with the active cases in Malaysia (Salman *et al.* 2021)

Figure 4 shows the results of the comparison of the active case and the SIR model used in (Salman *et al.* 2021). It can be seen that the result in Figure 3 differs slightly from the result in Figure 4, even though both models share much resemblance as both were able to capture the vital trend in the real data. The decrepancy in the result can be attributed to the difference in numerical methods used in obtaining the solution to the compartmental model that models the SIR.

The output from our hybrid model closely aligns with the results from the ode45 simulation. This strong resemblance suggests that our hybrid model successfully captures the key trends in real-world data. Both Figure 3 and Figure 5 display similar behavior, as each model effectively tracks the important dynamics observed in the real-world data. There are no obvious discrepancies between the results obtained using our hybrid model and the ode45 simulation in solving the underlying compartmental SIR model.

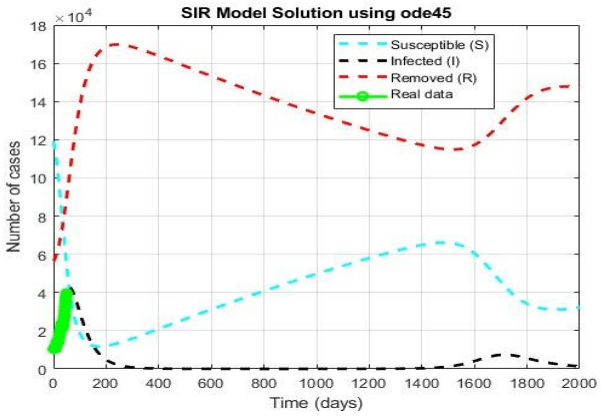

Figure 5: The numerical simulation results of our SIR model using the ode45 solver

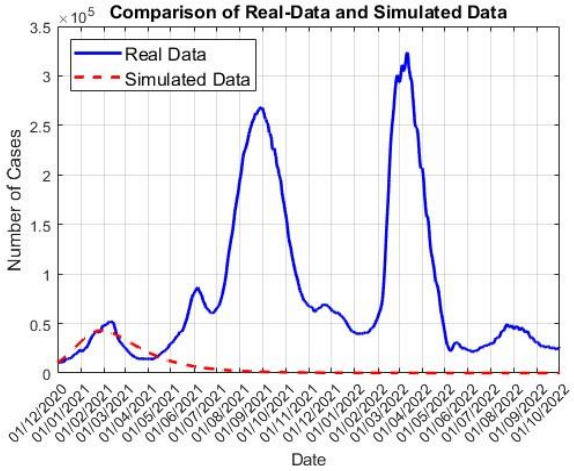

Figure 6: Actual infected cases in Malaysia and the prediction of the SIRS model generated by the 3-step ABM predictor-corrector method in the interval between December 1, 2020 till October 31, 2022

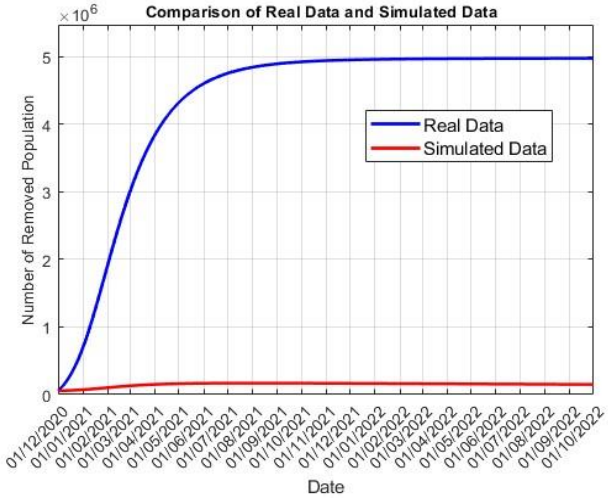

Figure 7: Actual removed cases in Malaysia and the prediction of the SIRS model generated by the 3-step predictor-corrector method in the interval between December 1, 2020 till October 31, 2022

Figures 6 and 7 demonstrate the dynamic of the real data and the predicted value for the infected population and recovery population, respectively. The real data peaked at various instances within the interval of interest but never returned to zero, and the predicted number of infected individuals is much smoother and lower than the actual data. The model predicts an initial rise in infections followed by a steady decline, with no major resurgence. We observe a significant difference between the SIRS model's predictions and the actual data for infected and removed cases in Malaysia. In other words, the model underestimates the infection peaks observed in the real data, indicating that it does not capture the intensity or frequency of the actual waves observed during the pandemic. This is because the SIRS model considered in this context incorporates a constant transmission rate, a constant recovery rate, and a relatively low reinfection force. Additionally, the model relies on the assumption of no medical resources, which means it doesn't account for factors like medical interventions or resources to mitigate the spread of the disease. Medical intervention, among many other factors, can make the model's predictions less plausible when compared to the actual data. The parameter values used in the SIRS model may not accurately reflect the specific circumstances of the COVID-19 outbreak in Malaysia.

We consider this hybrid a successful one because the hybrid model has proven to be efficient. It achieves this by capturing intelligent trends present in the data. In other words, the model is able to discern patterns, correlations, and significant features in the data that contribute to a better understanding of the phenomenon being studied. It also demonstrates the influence or impact of medical resources in retarding the spread of the COVID-19 disease. This suggests that the model can incorporate variables related to medical interventions, resources, or healthcare systems and evaluate their effectiveness in mitigating the spread of the disease. In a similar light, the model may be modified to offer better predictions that are more precise or realistic by incorporating the effectiveness of a treatment, immunisation rates, hospital capacity, and other pertinent variables that can influence the dynamics of the disease as medical variables. Furthermore, the quality of the data used to calibrate the model and estimate the parameter values plays a crucial role in the precision of the model's predictions. This suggests that if there are improvements in health screening or increased testing capacity, more active cases (including asymptomatic cases) will be reported, and effective strategies will be adopted to curb the situation and hinder the spread of the diseases among the susceptible population.

9. Conclusion

We utilised the SIRS model to analyse COVID-19 transmission dynamics in Malaysia. The SIRS model was solved using a hybrid model that combines the Runge-Kutta 4th order (RK4) method with the 3-step Adams-Bashforth-Moulton predictor-corrector technique. Simulations were carried out in MATLAB. Our findings suggest a fading chance of a resurgence of COVID-19 cases with diminishing immunity and a relatively low reinfection rate. The research shows that while the initial outbreak causes a large spike in infected cases, subsequent waves may occur as immunity wanes. This emphasises the importance of ongoing public health measures to manage the disease. However, our model’s projections did not perfectly match Malaysia's daily active and recovered cases, likely due to improved medical facilities in the country. Factors, including the availability of advanced medical facilities, which were not fully accounted for in the model, can significantly affect the accuracy of pandemic transmission forecasts. In addition, we found that, in spite of using the same parameter values, our forecast of the COVID-19 transmission tendency differs slightly from the SIR model used by Salman *et al.* (2021). This can be a result of differences in the

numerical techniques employed to conduct the research. By contrasting the anticipated and actual cases of infection and removal in the period from December 1, 2020, to October 31, 2022, it follows the same trend as most research conducted in the area. Epidemiological concepts such as false detection, face masks, and social distancing were classified as non-medical parameters to forecast the pandemic transmission dynamics since the research was conducted to visualise the depth of the impact of the transmission rate when there are no or limited medical facilities. Although this research can also be used to describe the impact of medical facilities in retarding the transmission of infectious diseases by observing the relation between affinity and difference when there are medical facilities and when we do not have such facilities or their availability is limited. In the future, we want to integrate this model into neural networks to solve constraint optimisation problems.

Acknowledgement

This research was supported by the School of Mathematical Sciences, Universiti Sains Malaysia.

References

Abdalla W., Renukappa S. & Suresh S. 2023. Managing COVID 19 related knowledge: A smart cities perspective. *Knowledge and Process Management* **30**(1): 87-109.

Ahmed A., Salam B., Mohammad M., Akgül A. & Khoshnaw S.H.A. 2020. Analysis coronavirus disease (COVID-19) model using numerical approaches and logistic model. *AIMS Bioengineering* **7**(3): 130-146.

Akinsola V. 2023. Numerical Methods: Euler and Runge-Kutta. In Shah K., Carpentieri B. & Ali A. (eds.). *Qualitative and Computational Aspects of Dynamical Systems*. London, UK: IntechOpen.

Akogwu B.O. & Fatoba J.O. 2022. Numerical solutions of COVID-19 SIRD model in Nigeria. *FUDMA Journal of Sciences* **6**(4): 60-67.

Alsayed A., Sadir H., Kamil R. & Sari H. 2020. Prediction of epidemic peak and infected cases for COVID-19 disease in Malaysia, 2020. *International Journal of Environmental Research and Public Health* **17**(11): 4076.

Asadi-Mehregan F., Assari P. & Dehghan M. 2023. The numerical solution of a mathematical model of the Covid-19 pandemic utilizing a meshless local discrete Galerkin method. *Engineering with Computers* **39**: 3327-3351.

Brauer F. 2017. Mathematical epidemiology: Past, present, and future. *Infectious Disease Modelling* **2**(2): 113-127.

Camacho A., Kucharski A., Aki-Sawyerr Y., White M.A., Flasche S., Baguelin M., Pollington T., Carney J.R., Glover R., Smout E., Tiffany A., Edmunds W.J. & Funk S. 2015. Temporal changes in Ebola transmission in Sierra Leone and implications for control requirements: a real-time modelling study. *PLoS Currents* **7**.

Chen T.M., Rui J., Wang Q.-P., Zhao Z.-Y., Cui J.-A. & Yin L. 2020. A mathematical model for simulating the phase-based transmissibility of a novel coronavirus. *Infectious Diseases of Poverty* **9**(1): 24.

Chen Z., Feng L., Lay Jr H.A., Furati K. & Khaliq A. 2022. SEIR model with unreported infected population and dynamic parameters for the spread of COVID-19. *Mathematics and Computers in Simulation* **198**: 31- 46.

Dong E., Du H. & Gardner L. 2020. An interactive web-based dashboard to track COVID-19 in real time. *Lancet Infectious Diseases* **20**(5): 533-534.

Giri A.K. & Rana D.R. 2020. Charting the challenges behind the testing of COVID-19 in developing countries Nepal as a case study. *Biosafety and Health* **2**(2): 53-56.

Hashim J.H., Adman M.A., Hashim Z., Mohd Radi M.F. & Kwan S.C. 2021. COVID-19 epidemic in Malaysia: epidemic progression, challenges, and response. *Frontiers in Public Health* **9:** 560592.

Kissler S.M., Tedijanto C., Goldstein E., Grad Y.H. & Lipsitch M. 2020. Projecting the transmission dynamics of SARS-CoV-2 through the postpandemic period. *Science* **368**(6493): 860-868.

Kraemer M.U.G., Hay S.I., Pigott D.M., Smith D.L., Wint G.R.W. & Golding N. 2016. Progress and challenges in infectious disease cartography. *Trends in Parasitology* **32**(1): 19-29.

Mohammed D.A., Tawfeeq H.M., Ali K.M. & Rostam H.M. 2021. Analysis and prediction of COVID-19 outbreak by a numerical modelling. *Iraqi Journal of Science* **62**(5): 1452-1459.

Mohd M.H. & Sulayman F. 2020. Unravelling the myths of R_0 in controlling the dynamics of COVID-19 outbreak: A modelling perspective. *Chaos, Solitons & Fractals* **138**: 109943.

Palma D.I. & Mungkasi S. 2024. Fourth and fifth-order Runge-Kutta methods for solving a susceptible-exposed-infected-recovered mathematical model of the spread of COVID-19. *AIP Conference Proceedings* **3074**: 020006.

Salman A.M., Ahmed I., Mohd M.H., Jamiluddin M.S. & Dheyab M.A. 2021. Scenario analysis of COVID-19 transmission dynamics in Malaysia with the possibility of reinfection and limited medical resources scenarios. *Computers in Biology and Medicine* **133**: 104372.

Shah A.U.M., Safri S.N.A., Thevadas R., Noordin N.K., Abd Rahman A., Sekawi Z., Ideris A. & Sultan M.T.H. 2020. COVID-19 outbreak in Malaysia: Actions taken by the Malaysian government. *International Journal of Infectious Diseases* **97**: 108-116.

Tang L., Zhou Y., Wang L., Purkayastha S., Zhang L., He J., Wang F. & Song P.X. 2020. A review of multi-compartment infectious disease models. *International Statistical Review* **88**(2): 462-513.

Viguerie A., Lorenzo G., Auricchio F., Baroli D., Hughes T.J.R., Patton A., Reali A., Yankeelov T.E. & Veneziani A. 2021. Simulating the spread of COVID-19 via a spatially-resolved susceptible–exposed–infected–recovered–deceased (SEIRD) model with heterogeneous diffusion. *Applied Mathematics Letters* **111**: 106617.

Yang C.Y. & Wang J. 2020. A mathematical model for the novel coronavirus epidemic in Wuhan. China. *Mathematical Biosciences and Engineering* **17**(3): 2708-2724.

Zhang P., Feng K., Gong Y., Lee J., Lomonaco S. & Zhao L. 2022. Usage of compartmental models in predicting COVID-19 outbreaks. *The AAPS Journal* **24**(5): 98.

Zhou L. & Fan M. 2012. Dynamics of an SIR epidemic model with limited medical resources revisited. *Nonlinear Analysis: Real World Applications* **13**(1): 312-324.

Zou L., Ruan F., Huang M., Liang L., Huang H., Hong Z., Yu J., Kang M., Song Y., Xia J., Guo Q., Song T., He J., Y. H.-L., Peiris M. & Wu J. 2020. SARS-CoV-2 viral load in upper respiratory specimens of infected patients. *The New England Journal of Medicine* **382**(12): 1177-1179

School of Mathematical Sciences
Universiti Sains Malaysia
11800 USM Penang, Malaysia
E-mail: salaudeenadebayo@gmail.com, saratha@usm.my[*]*, majidkhanmajaharali@usm.my, chenchuyi@student.usm.my, shinyinglim1014@student.usm.my*

School of General and Foundation Studies
AIMST University
08100 Bedong Kedah,
Malaysia
E-mail: dsmuraly@yahoo.com

Received: 24 August 2024
Accepted: 9 October 2024

[*]Corresponding author